

Accepted Manuscript

Development of a kinetic model of ethylene methoxycarbonylation with homogeneous Pd catalyst using a capillary microreactor

Federico Galvanin, Chara Psyrraki, Trevor Morris, Asterios Gavriilidis

PII: S1385-8947(17)30603-4

DOI: <http://dx.doi.org/10.1016/j.cej.2017.04.059>

Reference: CEJ 16813

To appear in: *Chemical Engineering Journal*



Please cite this article as: F. Galvanin, C. Psyrraki, T. Morris, A. Gavriilidis, Development of a kinetic model of ethylene methoxycarbonylation with homogeneous Pd catalyst using a capillary microreactor, *Chemical Engineering Journal* (2017), doi: <http://dx.doi.org/10.1016/j.cej.2017.04.059>

This is a PDF file of an unedited manuscript that has been accepted for publication. As a service to our customers we are providing this early version of the manuscript. The manuscript will undergo copyediting, typesetting, and review of the resulting proof before it is published in its final form. Please note that during the production process errors may be discovered which could affect the content, and all legal disclaimers that apply to the journal pertain.

Development of a kinetic model of ethylene methoxycarbonylation with homogeneous Pd catalyst using a capillary microreactor

Federico Galvanin^a, Chara Psyrraki^a, Trevor Morris^b, Asterios Gavriilidis^{a,*}

^a Department of Chemical Engineering, University College
London, Torrington Place, London, WC1E 7JE, UK

^b Lucite International, Wilton Centre, Wilton, Redcar, TS10 4RF, UK

*Corresponding author: a.gavriilidis@ucl.ac.uk

Abstract

The kinetics of gas-liquid methoxycarbonylation of ethylene using 0.0013 mol/L Pd(d^hbpx)(dba) homogeneous catalyst at 100°C and 10 bar were studied in a continuous flow Hastelloy capillary microreactor of 1 mm internal diameter. Characterisation of the hydrodynamics was conducted to confirm plug flow behaviour and evaluate liquid volume fraction, both important for reactor modelling. Reaction experiments were carried out to investigate the effect of ethylene, methanol and carbon monoxide concentrations on the observed reaction rate. Vapour-liquid equilibrium was employed to calculate component concentrations at the inlet and outlet reactor conditions from the experimental data. In conjunction with a reactor model, the results were used to evaluate kinetic models based on the Pd-hydride catalytic cycle. A kinetic model considering methanolysis as the rate limiting step agreed with the experimental data. A model-based design of experiments strategy was applied for selecting the most informative experiments to achieve a precise estimation of the kinetic model parameters.

Keywords: Kinetics, multiphase reactor, gas-liquid flow, kinetic modelling

1. Introduction

Methyl methacrylate (MMA) is one of the world's most important intermediates produced annually on a multi-million tonne scale and represents an essential component for acrylic-based products, such as resins and adhesives [1]. MMA is mainly produced via the acetone cyanhydrin (ACH) route, which requires careful management of large quantities of extremely toxic hydrogen cyanide and generates large amounts of acidic ammonium bisulphate waste, which has to be recovered by incineration at considerable cost. Recently, greener and more sustainable routes to MMA production have been developed [2] for minimising the impact of waste management on process economy. Among these routes, the Alpha Process for the production of MMA, recently developed by Lucite International, represents a greener route, involving no by-products and milder operating conditions and having ~40% less production costs compared to the ACH route [3].

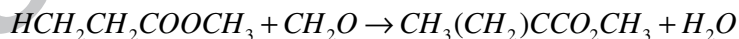
Two reaction stages are involved in the Alpha Process:

1) Ethylene methoxycarbonylation:



where methyl propionate ($HCH_2CH_2COOCH_3$, MeP) is synthesised via carbonylation and esterification of ethylene over Pd-based homogeneous catalyst;

2) Methyl methacrylate synthesis



where MeP reacts with formaldehyde (CH_2O) over Cs-based catalysts to form MMA.

The study of the aforementioned reaction stages through the development of reliable kinetic models is essential for process optimisation and design purposes. Flow systems represent an ideal environment for kinetic studies, as data can be obtained faster and with more precision than in batch systems [4]. Flow capillary microreactors

in particular have proven to be a powerful tool for studying kinetics in flow in multiphase systems [5-6] due to the high mass and heat transfer rates they provide, enabling the study of reactions that previously were difficult to investigate in conventional reactors. Furthermore, the use of microreactors is more cost effective compared to conventional reactors, and the amount of catalyst required is lower due to the small dimensions of the system [7].

The goal of the current work is the investigation of the reaction kinetics of the first stage of the Alpha Process, for the synthesis of methyl propionate (MeP) from ethylene, carbon monoxide and methanol over a homogenous Pd catalyst in a flow capillary microreactor. A two-step procedure was utilised. In the first step, the catalytic reaction was studied at the temperature and pressure typically used in industry (100°C, 10 bara) in a reactor system designed based on hydrodynamic studies that ensured favourable dispersion and mass transfer characteristics, allowing a discrimination between candidate kinetic models. In the second step, a one-dimensional tubular reactor model was developed using the gPROMS modelling platform [8] and was employed to select the most informative experimental data for the precise estimation of kinetic parameters according to a ranking of experiments approach [9]. In this second step, a wider range of reactants concentration was investigated in the experiments. The procedure guaranteed a statistical significance in parameter estimation and the accurate description of the experimental system behaviour under industrial operating conditions.

2. Experimental apparatus and procedure

The kinetic experiments were performed at 100°C, 10 bara. In Fig.1 the schematic for the set-up used is shown. Flowrates of ethylene, carbon monoxide and helium were

controlled by three mass flow controllers (Brooks 5850), while liquid flowrate was controlled by a high pressure syringe pump (KdS) and an 8 ml stainless steel syringe. Upstream of each mass flow controller and downstream of the syringe pump 10 μ m filters were installed. Downstream of the mass flow controllers check valves were installed to prevent any liquid backflush.

Gas and liquid flowrates were kept constant at 0.1ml/min (25°C, 10bara) and 0.005ml/min respectively. A 99:1 v/v MeP:MeOH solution was provided by Lucite International containing the catalyst [Pd(d^hbpx)(dba)] (dba=trans,trans-(PhCH=CH)₂CO). The catalyst solution was diluted with methanol and methyl propionate to the desired concentration. This was performed in a glove box under argon atmosphere to avoid any catalyst deactivation by contact with air. The solutions of methanol and methyl propionate used were first degassed with argon to remove any dissolved oxygen. The catalytic mixture consisted of 1:5:450 (molar ratios) Pd:Ligand:Methanesulfonic acid. The Pd concentration was 1.3·10⁻³ mol/L in all cases. The liquid stream was added to the ethylene stream via a T-junction and flowed through a pre-treatment section at 100°C. The pre-treatment section consisted of a 2m long Hastelloy capillary with 1.75mm inner diameter and 3.175mm outer diameter. After the pre-treatment section, carbon monoxide was introduced via a T-junction and the gas-liquid mixture entered the reactor at 100°C where the reaction began. The reactor was a 6m long Hastelloy capillary with 1mm inner diameter and 1.587mm outer diameter, providing an inert internal surface. Both capillaries for pre-treatment and reaction were inside an oil bath with a stirrer, placed on a hot plate to ensure uniform temperature. After the reactor, the gas-liquid mixture entered a gravity-based separator made of stainless steel. The liquid exited from the bottom of the separator,

where a metering valve helped to achieve controlled liquid sampling, while minimising pressure disturbance in the reactor. The pressure was monitored by means of a pressure transducer at the inlet of the reactor and kept constant at 10bara via a back pressure regulator (Brooks 5866) placed at the gas outlet after the liquid separator. The set-up was regularly checked for leaks by pressurising at 12 bar with helium.

Quantitative analysis of the gas and liquid reaction products was performed by a gas chromatograph (Agilent 7890A) using an online sampling valve and an auto-injector respectively. For the liquid analysis a mid-polar capillary column (DB-624, 30m x 320 μ m x 0.25m, Agilent) was used. In addition, a 2m long guard column of the same material with the main column was added before the main column to protect it from the acidic nature of the liquid samples. The liquid samples were analysed by an FID detector. For the gas analysis a polar capillary column (HP-Plot Q, Agilent) and a TCD detector were used. The experimental error for gas phase analysis was 0.5% and for liquid phase analysis was 2%.

3. Reactor model

Since it was not possible to measure component concentrations at the inlet and outlet of the reactor (100°C, 10 bara), a vapour-liquid equilibrium (VLE) model was used to calculate these from the specified and measured experimental data (25°C, 1 bara). A reactor model was developed in the gPROMS platform [8] and coupled with Multiflash for the description of VLE in the system. The reactor model was based on the following assumptions: plug flow, steady state isothermal conditions, constant gas and liquid volumetric flowrates. For each component the following mass balances in the liquid and the gas phase were considered:

$$\frac{1}{A_c} \frac{dF_i^l}{dz} = \nu R \varepsilon_l + k_l a \left(\frac{C_i^g}{K_i^{eq}} - C_i^l \right) \quad (1)$$

$$\frac{1}{A_c} \frac{dF_i^g}{dz} = -k_l a \left(\frac{C_i^g}{K_i^{eq}} - C_i^l \right) \quad (2)$$

where C_i^g and C_i^l are the concentrations (mol/mL), F_i^l and F_i^g are the molar flowrates (mol/min) of component i (MeOH, MeP, CO, C₂H₄) in the liquid and in the gas phase respectively, z is the distance (cm) in the axial coordinate, A_c is the reactor cross sectional area (cm²), ν is stoichiometric coefficient (equal to -1 for the reactants and 1 for the products), R is the reaction rate (mol ml⁻¹ min⁻¹), ε_l is the liquid volume fraction, $k_l a$ is the mass transfer coefficient (min⁻¹) considered constant for all components and K_i^{eq} is the gas-liquid equilibrium constant. The boundary conditions for Eq.1 and Eq.2 are given by the molar flowrates of all components at the inlet of the reactor.

For the determination of the mass transfer coefficient $k_l a$ the correlation proposed by Yue et al. [10] for slug-annular flow was used:

$$Sh \cdot \alpha \cdot d_H = 0.058 Re_g^{0.344} Re_l^{0.912} Sc^{0.5} \quad (3)$$

where Sh is the Sherwood number, Re_g and Re_l are Reynolds numbers for the gas and liquid phase respectively, Sc is the Schmidt number, d_H is the hydraulic diameter (m).

The liquid volume fraction value, ε_l was determined through residence time distribution experiments described in Section 4. The values of the gas-liquid equilibrium constants K_i were calculated by using the following equations:

$$K_i = \frac{\gamma_i H e_i}{\phi_i^v P^{tot}} \quad (4)$$

$$K_i = \frac{\gamma_i P_i^{vap}}{\phi_i^v P^{tot}} \quad (5)$$

where γ_i is the activity coefficient (-), He_i is the Henry's constant (bar), P_i^{vap} is the vapour pressure (bar) of component i , P^{tot} is the total gas pressure (bar) and ϕ_i^v is the fugacity coefficient (-) of the i -th component in the mixture. In Eqs. 4-5 the values for He_i reported in [11] were used. UNIQUAC correlations were adopted for evaluating the activity coefficients γ_i , while the Soave-Redlich-Kwong equation of state was used for calculating the fugacity coefficients ϕ_i^v . Eq.4 was used for carbon monoxide and ethylene, while Eq.5 was used for methanol and methyl propionate for conditions at the reactor inlet. It was then assumed that the thermodynamic equilibrium along the reactor and hence K_i remained constant.

4. Hydrodynamic study

Residence time distribution (RTD) experiments were performed under conditions similar to the reaction experiments (CO:C₂H₄ = 1:9, 30%wt MeOH:MeP, 100°C, 10bara) by monitoring a step change in the concentration of the liquid solution to pure methanol (using a 6-port valve) in the outlet of the Hastelloy reactor using an IR optical sensor. The set-up used for the RTD experiments has been previously described in detail by Cantu-Perez et al. [12]. A gas:liquid ratio of 20 was used (close to the one realized in reaction experiments), where the set gas and liquid flow rates were (25°C, 10bara) $v_g = 0.2$ mL/min and $v_l = 0.01$ mL/min, resulting to flowrates at the reactor entrance (100°C, 10bara) of $v_g = 0.277$ mL/min and $v_l = 0.0083$ mL/min. Assuming a perfect step at the reactor inlet and fitting the residence time distribution curve to an axial dispersion model [13] the dispersion number, D/uL was found equal to 0.0062, supporting the assumption of plug flow, since $D/uL < 0.01$. Based on RTD

experiments the liquid fraction ε_l in the system, which affects the reaction time, was determined according to the following equation:

$$\tau_l = \varepsilon_l \frac{L}{j_l} \quad (6)$$

where τ_l is the average residence time (s) of the liquid in the reactor, L is the length of the reactor (m) and j_l is the liquid superficial velocity (m/s). The liquid fraction for the experimental conditions above was found to be 0.044, while the observed flow-pattern (by means of a microscope) in the feed of the set-up (25°C, 10bara), where the tubing was transparent (made of PFA with the same inner diameter), was slug-annular with elongated bubbles (>30cm long) and relatively short liquid slugs (<2mm long).

5. Formulation of candidate kinetic models

In terms of reaction mechanism, there are two potential routes to methyl propionate (MeP) synthesis (Fig. 2a):

- Hydride cycle (A): the cycle starts with insertion of ethylene in the palladium hydride bond forming an alkyl complex. Then, insertion of carbon monoxide is followed to produce an acyl complex. Last step is addition of methanol that produces methyl propionate and regenerates the palladium hydride.
- Methoxycarbonyl cycle (B): starts with insertion of carbon monoxide in the palladium methoxy bond. Then, ethylene is added in the Pd-carbon bond of the alkoxy carbonyl-palladium complex. The final step is the addition of methanol that produces methyl propionate and generates the initial alkoxy palladium complex.

Clegg et al. [14] and Eastham et al [15] showed that the palladium catalysed methoxycarbonylation of ethylene follows the hydride cycle (A) which represents the

predominant route to MeP formation. The Pd-hydride reacts with ethylene to form the alkyl complex $[\text{Pd}(\text{L-L})\text{CH}_2\text{CH}_3]^+$. The alkyl complex then reacts with carbon monoxide to form acyl complex $[\text{Pd}(\text{L-L})(\text{C}(\text{O})\text{Et})(\text{MeOH})]^+$. These two steps are believed to be at equilibrium. The acyl complex is very reactive and undergoes methanol nucleophilic addition to yield the product and regenerate the Pd-hydride complex. Eastham et al [15] provided more details for the hydride mechanism (Figure 2b) using palladium complexes of unidentate phosphines (e.g. $\text{P} = \text{PPh}_3$) in methanol in the presence of methanesulfonic acid. Each step in the hydride sequence starts with a 16 electron palladium species followed by co-ordination of one of the components ethylene, CO or methanol to give a more stable 18 electron palladium species and then subsequent reaction with the other co-ordinated species.

The formulation of kinetic models depends on which reaction step is considered as the rate determining step in the proposed reaction mechanism (i.e the methanolysis step, the addition of ethylene or the addition of carbon monoxide). Three kinetic models, reported in Table 1, have been developed and preliminarily examined with respect to how well they explain the experimental observations of the system.

The main assumptions for these models are the following: a) The Pd-Hydride cycle (A in Fig. 4) is the predominant cycle, b) The reverse reaction of the MeP decomposition resulting in the formation of CO, C_2H_4 and MeOH is negligible, c)

Quasi-steady-state approximation for the unstable catalytic intermediates: this will assume that the intermediate complexes formed are very reactive and they never accumulate to considerable amounts compared to the concentrations of the main reactants (i.e. carbon monoxide, ethylene and methanol).

For the sake of clarity the various intermediate complexes are named in the following way:

$$IntA = (L-L)Pd(H)]^+ \quad (7)$$

$$IntB = (L-L)Pd(CH_2CH_3)^+$$

$$IntC = (L-L)Pd(CO)(CH_2CH_3)]^+.$$

The Palladium concentration in the reaction system can be evaluated for the three proposed kinetic models from:

$$[Pd] = [IntA] + [IntB] + [IntC] \quad (8)$$

where the quantities in square brackets are the concentrations of the species in (mol/ml). After rearranging the kinetic expressions of Table 1 in terms of measurable quantities the following reaction rate equations can be written for the three candidate models:

$$R^{Model1} = \frac{K_1 \cdot K_3 \cdot k_2 \cdot [Pd] \cdot [CO] \cdot [C_2H_4] \cdot [MeOH]}{1 + K_3 \cdot [MeOH] + K_1 \cdot K_3 \cdot [MeOH] \cdot [C_2H_4]} \quad (9)$$

$$R^{Model2} = \frac{K_3 \cdot K_2 \cdot k_1 \cdot [Pd] \cdot [CO] \cdot [C_2H_4] \cdot [MeOH]}{1 + K_2 \cdot [CO] + K_3 \cdot K_2 \cdot [CO] \cdot [MeOH]} \quad (10)$$

$$R^{Model3} = \frac{K_1 \cdot K_2 \cdot k_3 \cdot [Pd] \cdot [CO] \cdot [C_2H_4] \cdot [MeOH]}{1 + K_1 \cdot [C_2H_4] + K_1 \cdot K_2 \cdot [CO] \cdot [C_2H_4]} \quad (11)$$

6. Kinetic experiments and preliminary model discrimination

In order to study the reaction kinetics and discriminate among competitive kinetic models, $N = 41$ one-factor-at-a-time (OFAT) experiments were carried out to study the impact of reactants concentration on observed turnover frequency (TOF).

Experiments are grouped in the following way:

- Methanol (MeOH) series: 13 experiments with molar flowrate ranging from 40 to 115 $\mu\text{mol}/\text{min}$ (22-90%wt MeOH:MeP). CO partial pressure was kept constant at 1 bara, C_2H_4 partial pressure was kept constant at 9 bara.

- Carbon monoxide (CO) series: 16 experiments with molar flowrate ranging from 0.03 to 0.24 $\mu\text{mol}/\text{min}$ (CO partial pressure 0.5-4 bara). C_2H_4 partial pressure was kept constant at 5 bara, while the liquid feed was fixed at 30%wt MeOH:MeP.
- Ethylene (C_2H_4) series: 12 experiments with molar flowrate ranging from 0.32 to 2.15 $\mu\text{mol}/\text{min}$ (C_2H_4 partial pressure 2.3-8.3 bara). CO partial pressure was kept constant at 1 bara, while the liquid feed was fixed at 30%wt MeOH:MeP.

All the experiments were carried out at $T = 100^\circ\text{C}$ and $P = 10$ atm. Turnover frequency is defined as moles of MeP produced over moles of Pd over time. Experimental results are shown in Fig. 3. In Fig.3a the effect of CO on TOF is shown. CO has a positive effect on reaction rate. The order of reaction with respect to carbon monoxide is ca. 0.5 under the investigated conditions. This positive effect of CO has been observed in previous studies of alkene hydroformylation in a bubble column [16]. However, other studies showed that this dependence has a maximum, after which carbon monoxide inhibits the hydroformylation reaction due to catalyst poisoning [17]. This behaviour was not observed in our case, possibly because of the high concentration of the catalyst used. In Fig. 3b the C_2H_4 effect on TOF is shown. The observed order for ethylene concentration is zero, showing negligible effect of ethylene on reaction rate. In Fig. 3c the effect of methanol on TOF is shown for a fixed gas inlet stream of 10%v/v CO: C_2H_4 . A positive effect of methanol on reaction rate is shown with an observed order of about one. According to these experimental observations the only model which is compatible with the observed kinetics is Model 3 (whose reaction rate is given by Eq. 11). In fact, it can be observed that:

- According to Model 1 (Eq. 9), if $K_3 \cdot [\text{MeOH}] + K_1 \cdot K_3 \cdot [\text{MeOH}] \cdot [\text{C}_2\text{H}_4] \gg 1$ the denominator can be rewritten as $K_3 \cdot [\text{MeOH}] + K_1 \cdot K_3 \cdot [\text{MeOH}] \cdot [\text{C}_2\text{H}_4]$ and the reaction rate expression becomes

$$R^{Model1} = \frac{K_1 \cdot K_3 \cdot k_2 \cdot [Pd] \cdot [CO] \cdot [C_2H_4]}{K_3 + K_1 \cdot K_3 \cdot [C_2H_4]} \quad (12)$$

and the model becomes zero-order with respect to methanol. If

$K_3 \cdot [MeOH] + K_1 \cdot K_3 \cdot [MeOH] \cdot [C_2H_4] \ll 1$ the reaction rate becomes

$$R^{Model1} = K_1 \cdot K_2 \cdot k_3 \cdot [Pd] \cdot [CO] \cdot [C_2H_4] \cdot [MeOH] \quad (13)$$

and the increase on concentration of CO, methanol and ethylene should have a positive effect on reaction rate (first order dependency). Both cases contradict experimental observations.

- According to Model 2 (Eq. 10), a positive effect of ethylene on reaction rate is expected, which contradicts experimental observations.
- According to Model 3 (Eq. 11), ethylene can have no effect on the observed reaction rate, while methanol should have a positive effect, both consistent with experimental observations.

Model 3, where methanolysis represents the rate limiting step, is consistent with the experimental observations, being 0.5-order with respect to carbon monoxide, first order with respect to methanol and zero order with respect to ethylene. Hence, only Model 3 has been utilised in the reactor model.

6.1 Discussion on observed kinetics and hydride mechanism

According to the hydride mechanism proposed by Eastham and colleagues [15] (Figure 2b), if methanol addition represents the rate determining step, it is either the co-ordination of methanol or its subsequent reaction with the acyl species and elimination of methyl propionate that is rate limited. It seems more likely that the rates of co-ordination that are rate limiting rather than their subsequent intra molecular reaction, as this would involve a bi-molecular reaction mechanism. There

can be two possible explanations why nucleophilic reaction with methanol may be slower:

1. **Methanol activity:** methanol will tend to be hydrogen bonded to more methanol and will be at least partially protonated by the strong acid present. Protonated methanol molecules will be repelled by the charge on the complex and hydrogen bonded methanol molecules will have one of their oxygen lone pairs tied up and will also behave as a loose cluster.
2. **Steric effect:** the large phosphine ligand molecules attached to the complex restrict access to the Palladium (this can be used to explain why no further addition of ethylene and CO is observed to form oligomers rather than just forming MeP selectively). In this context, there may only be sufficient space around the Palladium for completely free methanol molecules to access it (the oxygen lone pair has to co-ordinate to the Palladium). So whilst the concentration of methanol is high, the availability of free methanol molecules capable of co-ordinating may be lower and hence the reaction is slower to occur.

7. Sensitivity analysis and parameter estimation

Based on the model described by Eqs 1-5 and the kinetic model given by Eq. 11, a preliminary estimation of kinetic parameters was performed. A sensitivity analysis was carried out on the parametric system (K_1 , K_2 , k_3) to verify the impact of parameter variation on the measured responses. A drawback of the kinetic model represented by Eq. 11 is that kinetic parameters K_1 and K_2 are practically not identifiable from experimental observations. In particular, as it can be seen from Fig. 4 (black bars in the graph), the sensitivity to MeP flowrate to these parameters is nearly zero at the conditions of the standard experiment (10%v/v CO:C₂H₄, 30%wt MeOH:MeP, 100°C,

10 bara). This poses severe model identifiability issues, hindering the estimation of the kinetic parameters in a statistically satisfactory way [18].

In order to improve the estimability of kinetic parameters, a model reparameterisation was applied to Eq. 11, which was reformulated as

$$R = \frac{C \cdot [Pd] \cdot [CO] \cdot [C_2H_4] \cdot [MeOH]}{1 + A \cdot [C_2H_4] + B \cdot [CO] \cdot [C_2H_4]} \quad (14)$$

by introducing the following equations

$$A = K_1 = A_n \cdot \theta_1 \quad (15)$$

$$B = K_1 \cdot K_2 = B_n \cdot \theta_2 \quad (16)$$

$$C = K_1 \cdot K_2 \cdot k_3 = C_n \cdot \theta_3 \quad (17)$$

In Eqs 15-17 A_n , B_n and C_n are normalisation factors introduced to avoid numerical issues due to the small numbers involved in the simulation ($A_n = 10^5$, $B_n = 1015$, $C_n = 2 \cdot 10^{18}$) while $\theta = [\theta_1 \ \theta_2 \ \theta_3]^T$ is the new set of parameters to be estimated. For the same reason, a scaling factor was introduced in the reaction rate (Eq. 14) by considering the transformation $R = D_n \cdot R_n$ with $D_n = 10^{18}$. The positive effect of kinetic model reparameterisation is evident by comparing the sensitivities of the original model (black bars in Fig. 4) with the ones of the reparameterised model (red bars).

Using the reparameterised model, the new set of parameters θ was estimated in gPROMS ModelBuilder [8] using a maximum likelihood parameter estimation technique. Flowrate errors were assumed normally distributed with a standard deviation of $\sigma_y = 3 \cdot 10^{-3}$ mmol/min. Parameter estimation results were analysed in terms of estimated values and statistics to quantify both the precision of the estimates (by analysing the standard deviation of the estimates and by using t -test statistics) and the fitting performance of the model (by using chi-square (χ^2) statistics). For a precise

parameter estimation, the t -value at the 95% confidence level of each kinetic parameter evaluated from

$$t_i = \frac{\hat{\theta}_i}{2\sigma_\theta} \quad (18)$$

should be higher than t^{ref} , a tabulated reference t -value given by a Student t -distribution with $(N - N_\theta)$ degrees of freedom. In Eq. 18 $\hat{\theta}_i$ is the estimated value and σ_θ is the estimated standard deviation of the i -th parameter obtained from maximum likelihood [19]. In order to assess the fitting performance, the chi-square statistics

$$\chi^2 = \sum_{i=1}^{N_y} \sum_{j=1}^{N_{sp}} \frac{(y_{ij} - \hat{y}_{ij})^2}{\sigma_{y_i}^2} \quad (19)$$

was computed and compared with χ_{Ref}^2 , a reference value from a χ^2 distribution with $(N - N_y)$ degrees of freedom (N is the total number of experimental points, N_y is the number of measured responses). In Eq. 19 y_{ij} is the j -th measurement of the i -th response, \hat{y}_{ij} is the corresponding model prediction, while $\sigma_{y_i}^2$ is the variance for the i -th measurement. For a satisfactory fitting performance the calculated χ^2 should be low and $\chi^2 < \chi_{Ref}^2$, meaning that the χ^2 test is positively passed.

Parameter estimation results are presented in Table 2. Parameters θ_2 and θ_3 were estimated with great accuracy, while the standard deviation in the estimation of parameter θ_1 still remains significant. This indicates that the precise estimation of the whole set of parameters in the experimentally investigated design space is not possible by using the full set of screening measurements. A detailed data mining based on information analysis is thus necessary to select only informative experiments for improving parameter estimation. Even though, based on these values of the parameters, the model was able to fit the full set of kinetic data in the whole design

space, the fitting was not statistically satisfactory, as underlined by the χ^2 test ($\chi^2 = 101.49 > 60.48 = \chi_{Ref}^2$), indicating a poor fitting performance.

8. Information analysis and ranking of experiments

In order to improve the precision on the estimation of parameter θ_l , an information analysis was carried out to quantify the relative amount of information which can be evaluated from each single experiment. This has been done by computing a metric function of the Fisher Information Matrix (FIM) for the model described by equations Eqs 1-5 and Eq. 11. For each experiment, the FIM \mathbf{H}_θ was evaluated at the set of experimental conditions $\boldsymbol{\varphi}$ and at the value $\boldsymbol{\theta}$ of the model parameters:

$$\mathbf{H}_\theta(\boldsymbol{\theta}, \boldsymbol{\varphi}) = \sum_{k=1}^{n_{sp}} \sum_{i=1}^{N_y} \sum_{j=1}^{N_y} s_{ij} \left[\frac{\partial \hat{y}_i(z_k)}{\partial \theta_l} \frac{\partial \hat{y}_j(z_k)^T}{\partial \theta_m} \right]_{l,m=1 \dots N_\theta}. \quad (20)$$

In Eq. 20, $\hat{y}_i(z_k)$ is the prediction of the i -th flowrate at the reactor outlet in the k -th experimental point and s_{ij} is the ij -th element of the $N_y \times N_y$ inverse matrix of measurements error. The term between square brackets represents the product between the sensitivities of each response to the model parameters. A Relative Fisher Information (RFI) index can be introduced based on the FIM definition [9] in order to evaluate the relative amount of information which can be obtained for the estimation of the model parameters from the i -th experiment

$$RFI_i = \frac{\sum_{j=1}^{N_y} \|\mathbf{H}_{ij}\|}{\sum_{i=1}^{N_{exp}} \sum_{j=1}^{N_y} \|\mathbf{H}_{ij}\|} = \frac{\|\mathbf{H}_i\|}{\|\mathbf{H}\|}. \quad (21)$$

In Eq. 21, $\|\mathbf{H}_{ij}\|$ and $\|\mathbf{H}_i\|$ are, respectively, the FIM related to the i -th experiment coming from the j -th response and the global information from the i -th experiment; $\|\mathbf{H}\|$ is the global information obtained from N_{exp} experiments for the identification of the model according to a suitable norm $\|\cdot\|$ (trace, determinant or maximum eigenvalue). In this study, the trace of FIM was used as a suitable matrix norm.

Based on RFI it is possible:

- To compute the best experimental conditions for estimating the kinetic parameters (these are the ones identified by the highest $\|\mathbf{H}_i\|$)
- To quantify the amount of information related to one or more experiments (allowing for ranking of performed experiments based on the relative contribution to the overall information)
- To quantify the amount of information associated to each measured variable (i.e. CO, MeOH, MeP or C₂H₄ flowrates) by evaluating the RFI for each response.

A selection algorithm was applied to discard non-informative experiments (i.e. experiments providing very low sensitivities of the kinetic parameters to the measured responses). The experimental conditions associated with these experiments is such that they do not provide a significant increase on the overall information $\|\mathbf{H}\|$. Results from RFI analysis are shown in Fig. 5. The computation of $\|\mathbf{H}_i\|$ for the full set of performed screening experiments is shown in Fig. 5a. It is apparent that a number of experiments provide a very low level of information. Hence, 13 experiments with $\|\mathbf{H}_i\| < \delta = 2 \cdot 10^{-2}$ were discarded from the model identification study¹. Furthermore, by analysing the contribution of each measured response in terms of RFI (Figure 5b)

¹ The value of the threshold δ has been chosen because the repetition of 41 experiments with this value of information would generate an average t -value of 0.01 on the model parameters, which is totally unsatisfactory for the purpose of parameter estimation.

it is evident that only MeOH and MeP measurements provide valuable information for the estimation of kinetic parameters, whilst the inclusion of CO and C₂H₄ measurements give a negligible increment to the overall information $\|\mathbf{H}\|$ (they only represent 0.08% of the overall information).

In Fig. 6 the experiments are ordered by information content (RFI calculated from Eq. 22) and labelled according to the experimental design (OFAT allocation) by using different colours. Among the 13 experiments discarded by the selection algorithm, 7 are experiments at variable ethylene concentration (blue bars), as this factor would not significantly change the measured responses. More importantly, the most informative experiments are the ones where CO concentration was altered (CO series), while experiments where ethylene was altered show a relatively low amount of information. By analysing the experimental conditions in terms of liquid inlet flowrate associated to the most and to the least informative experiments (experiment 133 and A6 respectively) (Table 3) it can be observed that the best operating conditions for the estimation of kinetic parameters are realised at low ethylene concentration and high CO concentration at moderate MeOH concentration.

9. Estimation of kinetic model parameters

The application of the selection algorithm based on ranking of reaction experiments decreased the overall number from $N_{exp} = 41$ to $N_{exp} = 28$ informative experiments. However, the impact of discarding 13 non-informative experiments on model validation is relevant. Parameter estimation results are shown in Table 4 in terms of new estimated values and statistics. The application of the algorithm allowed achieving a precise and statistically satisfactory parameter estimation of the full set of

kinetic experiments (including θ_1) as underlined by the analysis of the t -values and confidence intervals. Furthermore, the technique guarantees a good fitting of the experimental data, as shown by the χ^2 test, now amply satisfied (i.e. $\chi^2 = 52.05 < 60.48 = \chi_{Ref}^2$).

From the results of Table 4, given the reparameterisation carried out in the original model through Eqs 15-17, it is possible to calculate the kinetic parameters K_1 , K_2 and k_3 of the original model (Eq. 11). Results are given in Table 5 and show that $K_2 \gg K_1$, indicating a stronger affinity of CO for the catalyst. The fitting performance of the model in terms of experimentally observed reaction rate and MeOH and MeP outlet flowrate (liquid phase) are illustrated in Fig. 7a and Fig. 7b respectively by means of parity plots. A very good agreement in terms of reaction rate with the experimental results is observed, and the agreement with the liquid flowrate values is always within the 10% band of variability, suggesting a good performance of the model under the investigated experimental conditions.

5. Conclusions

A kinetic study of ethylene methoxycarbonylation was carried out in a capillary microreactor. A model identification strategy, aiming to link the experimental information with the modelling activity, was proposed for the development of kinetic models. The kinetic experiments showed that carbon monoxide and methanol have a positive effect on the reaction rate in the operating design space, while ethylene presented insignificant effect on the reaction rate. Based on the hydride cycle, a kinetic model of 0.5-order with respect to carbon monoxide, first order with respect to methanol and zero order with respect to ethylene, where methanolysis represents the rate limiting step, was found suitable to represent the experimental observations. A

one-dimensional plug flow reactor model of the capillary microreactor was then developed, including kinetics, mass transfer and the description of vapour-liquid equilibrium at the inlet/outlet of the reactor. A model reparameterisation and an information analysis were carried out to address parametric identifiability issues arising because of the poor sensitivity of the measured responses to the kinetic parameters. The procedure allowed achieving a statistically precise estimation of the full set of model parameters and a good representation of the experimental observations.

Acknowledgement. This work was supported by Lucite International and UCL. The authors would like to thank Graham Eastham, Darren Gobby, Neil Tindale, Neil Turner and Mark Waugh for their valuable contributions.

References

- [1] Bauer, W., 2002. Methacrylic Acid and Derivatives. In: Ullmann's Encyclopedia of Industrial Chemistry 2002, Wiley-VCH, Weinheim.
- [2] Andraos, J., 2016. Complete Green Metrics Evaluation of Various Routes to Methyl Methacrylate According to Material and Energy Consumptions and Environmental and Safety Impacts: Test Case from the Chemical Industry. *ACS Sustainable Chemical Engineering* 4, 312-323.
- [3] Clegg, W., Elsegood, M. R. J., Eastham, G. R., Tooze, R. P., Lan Wang, X., Whiston, K., 1999. Highly active and selective catalysts for the production of methyl propanoate via the methoxycarbonylation of ethane. *Chemical Communications* 1877-1878.

- [4] Al-Rifai, N., Cao, E., Dua, V., Gavriilidis A., 2013. Microtechnology technology aided catalytic process design. *Current Opinion in Chemical Engineering* 2, 338-345.
- [5] Tsoligkas, A. N., Simmons, M. J. H., Wood, J., Frost, C. G., 2007. Two phase gas-liquid reaction studies in a circular capillary. *Catalysis Today* 128, 36-46.
- [6] Jevtic, R., Ramachandran, P. A., Dudukovic, M. P., 2010. Capillary reactor for cyclohexane oxidation with oxygen. *Chemical Engineering Research and Design* 88, 255-262.
- [7] Poechlauer, P., Vorbach, M., Kotthaus, M., Braune, S., Reintjens, R., Mascarello, F., Kwant, G., 2009. *Micro Process Engineering* (V. Hessel, A. Renken, J.C. Schouten, J.-I. Yoshida, Eds.), Wiley-VCH, Weinheim, 3, 249-254.
- [8] Process Systems Enterprise, 2012. gPROMS model validation guide (v. 3.6). London: Process Systems Enterprise, 1-72.
- [9] Galvanin, F., Cao, E., Al-Rifai, N., Gavriilidis, A., Dua, V., 2016. A joint model-based experimental design approach for the identification of kinetic models in continuous flow laboratory reactors. *Computers and Chemical Engineering* 95, 202-215.
- [10] Yue, J., Chen, G., Yuan, Q., Luo, L., Gonthier, Y., 2007. Hydrodynamics and mass transfer characteristics in gas-liquid flow through a rectangular microchannel. *Chemical Engineering Science* 62, 2096-2108.
- [11] Torres, A., 2009. In situ measurement of gas concentrations in working catalytic reactors by HPNMR. PhD Thesis, University of Liverpool.
- [12] Cantu-Perez, A., Barrass, S., Gavriilidis, A., 2010. Residence time distributions in microchannels: comparison between channels with herringbone structures and a rectangular channel. *Chemical Engineering Journal* 160, 834-844.

- [13] Levenspiel, O., 1999. *Chemical Reaction Engineering*, John Wiley & Sons, London.
- [14] Clegg, W., Eastham, G. R., Elsegood, M. R. J., Heaton, B. T., Iggo, J. A., Tooze, R. P., Whyman, R., Zacchini, S., 2002. Synthesis and reactivity of palladium hydrido-solvento complexes, including a key intermediate in the catalytic methoxycarbonylation of ethene to methyl propanoate. *Journal of the Chemical Society, Dalton Transactions* 3300-3308.
- [15] Eastham, G. R., Tooze, R. P., Kilner, M., Foster, D. F., Cole-Hamilton, D. J., 2002. Deuterium labelling evidence for a hydride mechanism in the formation of methyl propanoate from carbon monoxide, ethene and methanol catalysed by a palladium complex, *Journal of the Chemical Society, Dalton Transactions* 1613-1617.
- [16] Torres, A., Molina Perez, N., Overend, G., Hodge, N., Heaton, B.T., Iggo, J.A., Satherley, J., Whyman, R., Eastham, G.R., Gobby, D., 2012. High-Pressure In Situ NMR Methods for the Study of Reaction Kinetics in Homogeneous Catalysis. *ACS Catalysis* 2, 2281-2289.
- [17] Wolowska, J., Eastham, G. R., Heaton, B. T., Iggo, J. A., Jacob, C., Whyman, R., 2002. The effect of mechanistic pathway on activity in the Pd and Pt catalysed methoxycarbonylation of ethene. *Chemical Communications* 2784-2785.
- [18] Galvanin, F., Ballan, C.C., Barolo, M., Bezzo F., 2013. A general model-based design of experiments approach to achieve practical identifiability of pharmacokinetic and pharmacodynamic models. *Journal of Pharmacokinetics and Pharmacodynamics* 40, 451-467.
- [19] Bard, Y., 1977. *Nonlinear parameter estimation*. Academic Press, New York (U.S.A.).

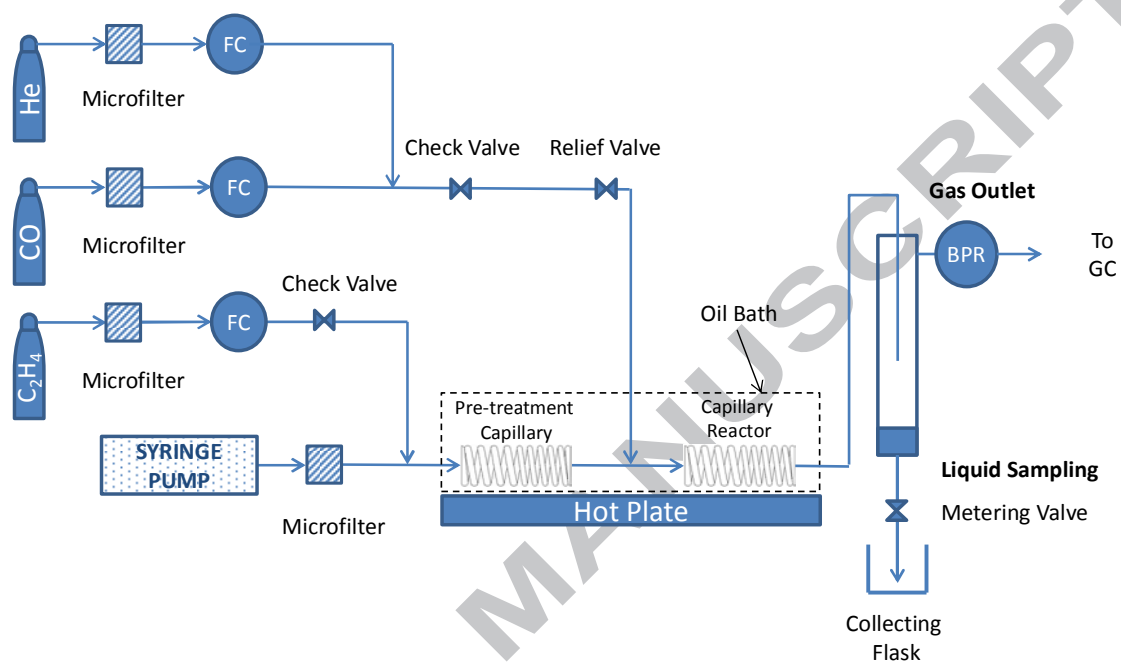


Fig.1 Schematic of the experimental set-up used for the kinetic study. FC: Mass flow Controller; BPR: Back Pressure Regulator; GC: Gas Chromatograph.

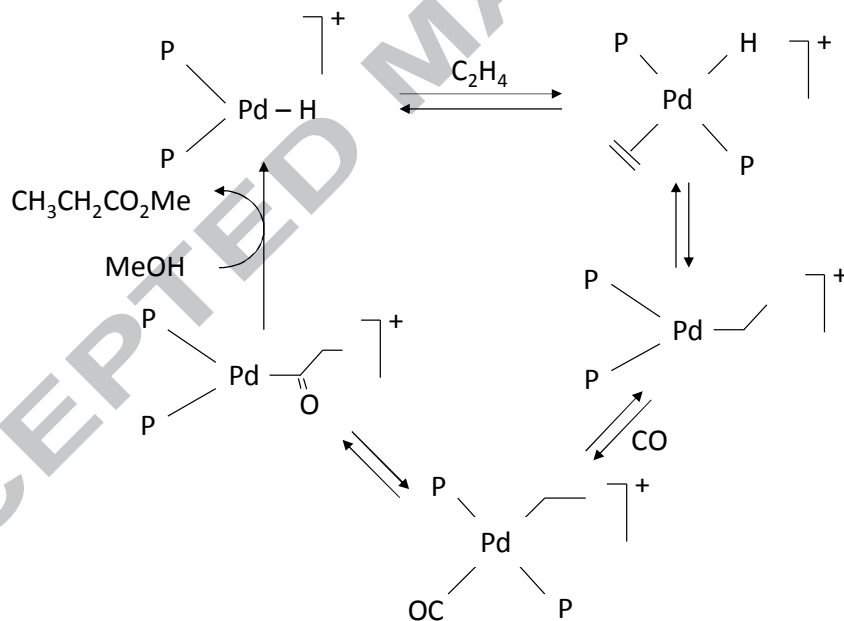
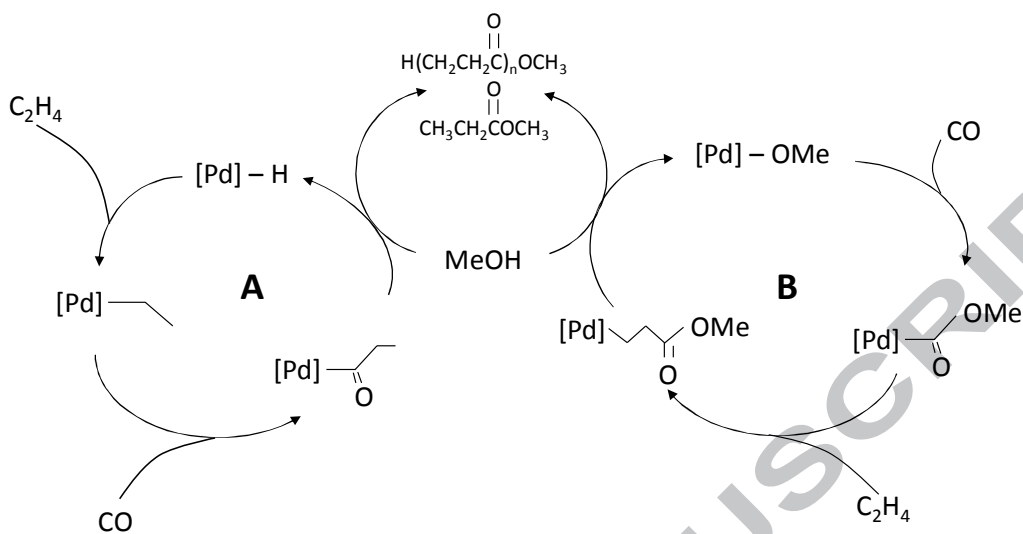
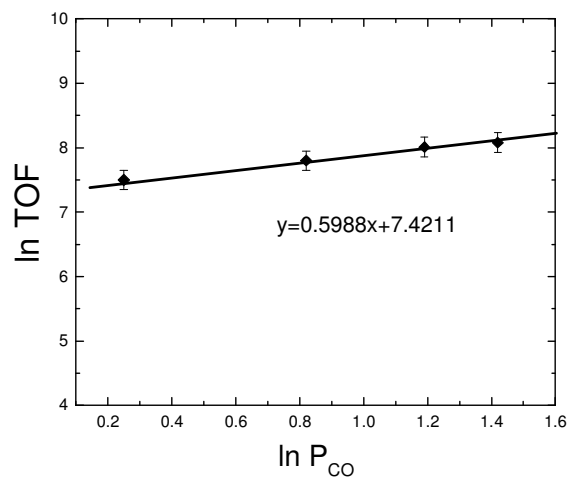
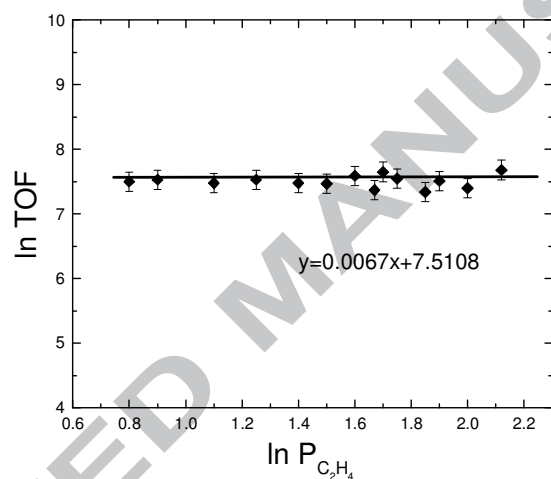


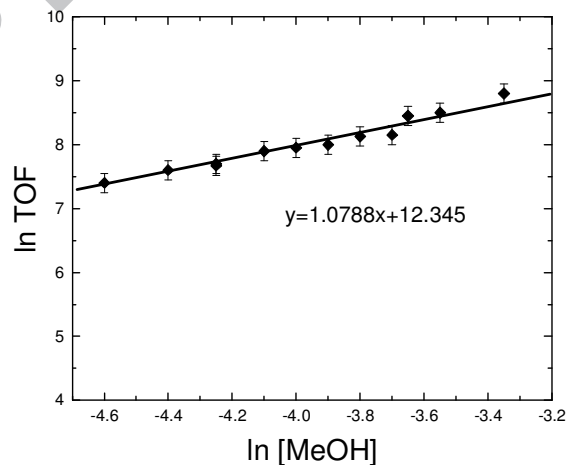
Fig.2 (a) Hydride cycle (A) and methoxycarbonyl cycle (B) for the synthesis of methyl propionate (MeP) as reported in [14]. (b) Hydride cycle mechanism for the synthesis of methyl propionate from methanol, ethene and CO using palladium complexes of unidentate phosphines (e.g. $P = PPh_3$) in the presence of methane sulfonic acid as proposed by Eastham and coworkers [15].



(a)



(b)



(c)

Fig. 3 (a) Effect of carbon monoxide concentration on turnover frequency (TOF) for a liquid feed stream of 30%wt MeOH:MeP and 50%vol C_2H_4 in the gas feed; (b) Effect of ethylene concentration on TOF for a liquid feed stream of 30%wt MeOH:MeP and 10%vol CO in the gas feed; (c) Effect of methanol concentration on TOF for a gas feed stream of 10%vol CO: C_2H_4 .

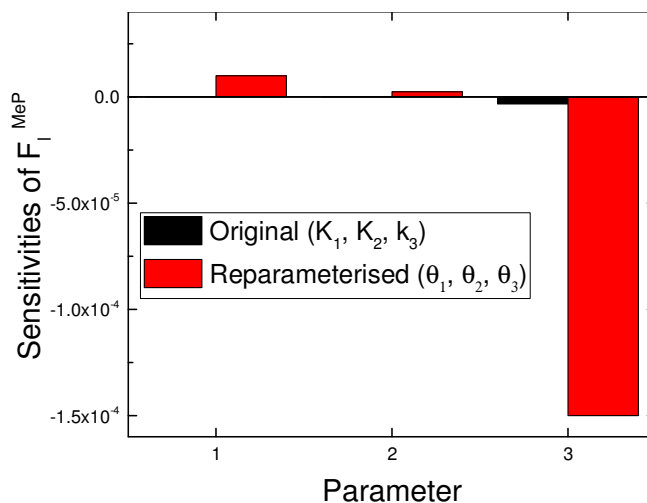
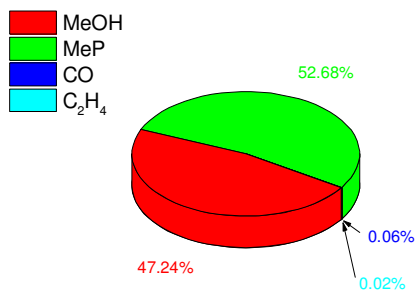
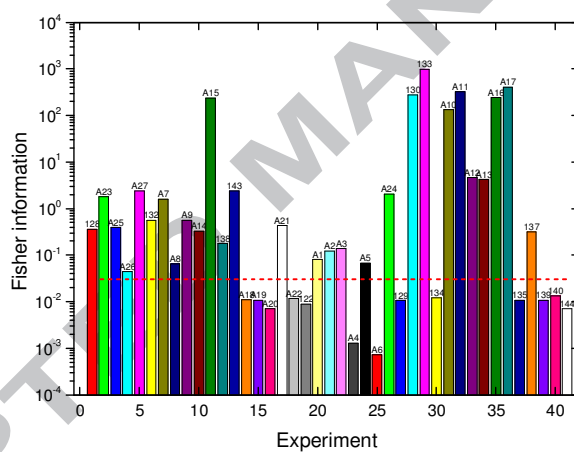


Fig. 4 Effect of model reparameterisation on the sensitivities to MeP flowrate evaluated at the standard experimental conditions (10%v/v $\text{CO}:\text{C}_2\text{H}_4$, 30%wt MeOH:MeP, 100°C , 10 bara).



(a)

(b)

Fig. 5 Information analysis for the full set of experiments performed at variable composition of the liquid feed stream. (a) Trace of the Fisher Information Matrix for the experiments performed (the information threshold is indicated by the broken red line); (b) Relative Fisher Information analysis on the measured responses (MeOH, MeP, CO, C_2H_4 outlet flowrates).

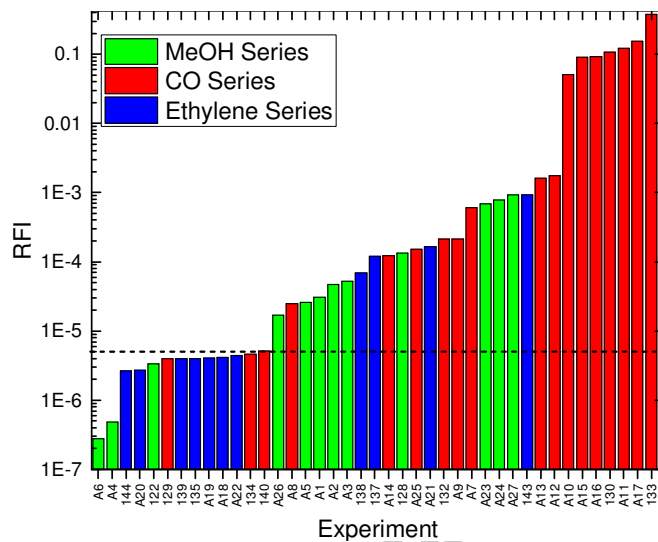
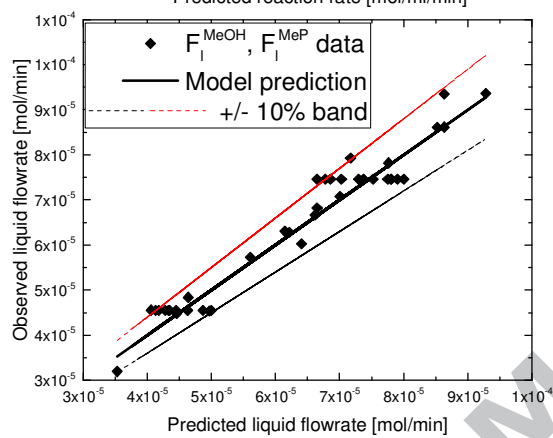
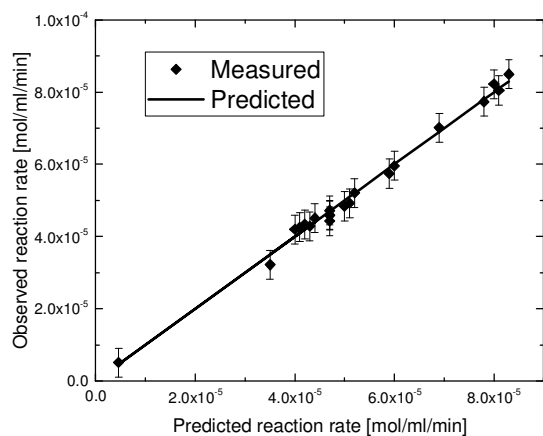


Fig. 6 Relative Fisher Information (RFI) analysis for the full set of experiments performed at variable composition of the liquid feed stream. Information threshold is indicated by the black broken line.



(a)

(b)

Fig. 7 Parity plots obtained after parameter estimation. (a) Observed reaction rate vs Predicted reaction rate; (b) Observed outlet liquid flowrates vs Predicted outlet liquid flowrates for MeOH and MeP. The $\pm 10\%$ variation band is indicated by thin broken lines.

Table 1 Proposed kinetic models based on different rate determining steps (the intermediate species are: $IntA = (L-L)Pd(H)J^+$; $IntB = (L-L)Pd(CH_2CH_3)^+$; $IntC = (L-L)Pd(CO)(CH_2CH_3)J^+$). In the kinetic models, k_i and K_i represent the reaction rate constant and the equilibrium constant of the i -th reaction.

Model	Rate determining step	Reactions	Kinetic expressions
Model 1	CO addition	$IntA + C_2H_4 \xrightleftharpoons{K_1} IntB$ $IntB + CO \xrightarrow{k_2} IntC$ $IntC + CH_3OH \xrightleftharpoons{K_3} IntA + CH_3CH_2COOCH_3$	$R = k_2 \cdot [IntB] \cdot [CO]$ $K_1 = \frac{[IntB]}{[IntA] [C_2H_4]}$ $K_3 = \frac{[IntA]}{[IntC] \cdot [MeOH]}$
Model 2	Ethylene addition	$IntA + C_2H_4 \xrightarrow{k_1} IntB$ $IntB + CO \xrightleftharpoons{K_2} IntC$ $IntC + CH_3OH \xrightleftharpoons{K_3} IntA + CH_3CH_2COOCH_3$	$R = k_1 \cdot [IntA] \cdot [C_2H_4]$ $K_2 = \frac{[IntC]}{[IntB] \cdot [CO]}$ $K_3 = \frac{[IntA]}{[IntC] [MeOH]}$
Model 3	Methanolysis	$IntA + C_2H_4 \xrightleftharpoons{K_1} IntB$ $IntB + CO \xrightleftharpoons{K_2} IntC$ $IntC + CH_3OH \xrightarrow{k_3} IntA + CH_3CH_2COOCH_3$	$R = k_3 \cdot [IntC] \cdot [MeOH]$ $K_1 = \frac{[IntB]}{[IntA] [C_2H_4]}$ $K_2 = \frac{[IntC]}{[IntB] \cdot [CO]}$

Table 2 Parameter estimation results for the reparameterised model including estimated value, standard deviation and 95% t-value. Parameters failing the t-test are indicated in boldface.

Parameter	Value	Standard Deviation	95% t-value
θ_1	0.04160	549.0011	$3.58 \cdot 10^{-5}$
θ_2	0.01028	0.0091	5.298
θ_3	0.00375	0.0003	5.309
Reference t-value (95%)			1.745
χ^2 ($\chi^2_{\text{ref}} = 60.48$)			101.49

Table 3 Experimental conditions of inlet liquid flowrate (mmol/min) for the most informative experiment (experiment 133) and the least informative experiment (experiment A6) according to RFI analysis. The maximum and minimum values of the flowrates used in the experiments are also provided for clarity.

Species in the feed stream	Liquid flowrate in the feed (mol/min)			
	133	A6	Min. Value	Max. Value
MeOH	5.56E-5	4.86E-5	4.00E-5	1.15E-4
CO	2.44E-7	6.30E-8	2.85E-8	2.44E-7
C ₂ H ₄	8.88E-7	1.98E-6	3.18E-7	2.17E-6
RFI	0.37	2.78E-7	-	

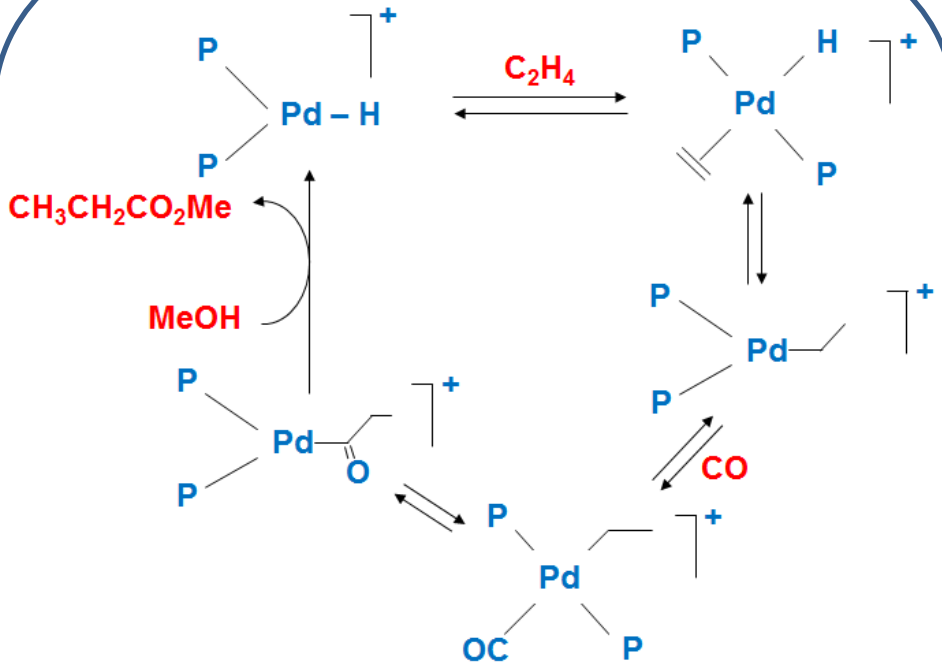
Table 4 Parameter estimation results for the reparameterised model after the application of the selection algorithm based on ranking of experiments. Results include estimated value, standard deviation and 95% t-value. Values in parenthesis are the parameter estimation results obtained from the full set of experiments for the sake of comparison. Parameters failing the t-test are indicated in boldface.

Parameter	Final Value	Standard Deviation	95% t-value
θ_1	9.798E-6 (0.0416)	5E-6 (549.0011)	1.701 ($3.58 \cdot 10^{-5}$)
θ_2	0.1049 (0.1028)	0.0048 (0.0091)	10.881 (5.298)
θ_3	0.0041 (0.0037)	0.0002 (0.0003)	10.942 (5.309)
Reference t-value (95%)			1.680 (1.745)
χ^2 ($\chi^{2, \text{ref}} = 60.48$)			52.05 (101.49)

Table 5 *Estimated values of the parameters k_3 , K_1 , K_2 in the original kinetic model (Eq. 11).*

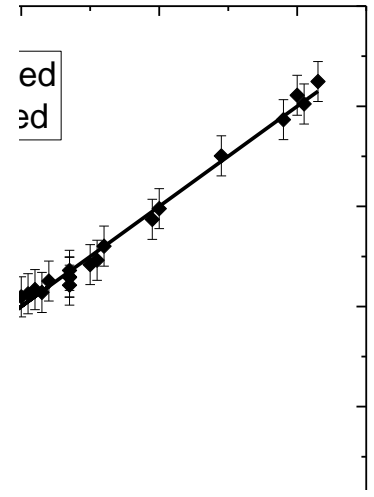
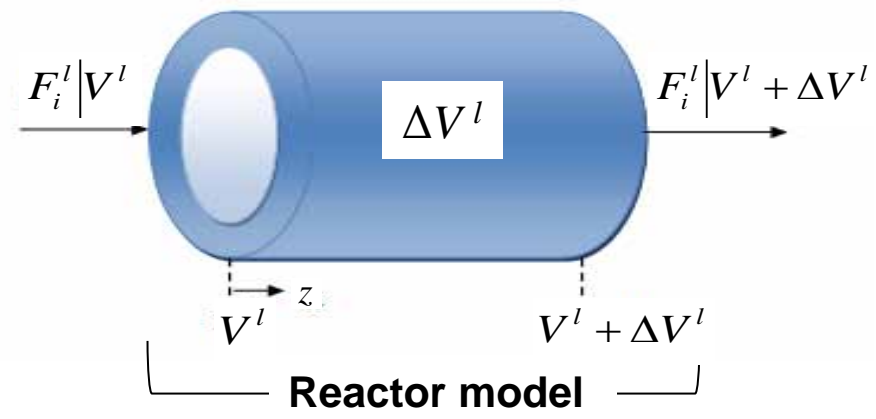
Parameter	Final Value
k_3 [mL/mol/min]	7.913E01
K_1 [mL/mol]	9.791E04
K_2 [mL/mol]	1.071E9

ACCEPTED MANUSCRIPT



Kinetic model

$$R = \frac{K_1 \cdot K_2 \cdot k_3 \cdot [\text{Pd}] \cdot [\text{CO}] \cdot [\text{C}_2\text{H}_4] \cdot [\text{MeOH}]}{1 + K_1 \cdot [\text{C}_2\text{H}_4] + K_1 \cdot K_2 \cdot [\text{CO}] \cdot [\text{C}_2\text{H}_4]}$$



Highlights

- Kinetics of ethylene methoxycarbonylation was studied in a capillary reactor
- The methanolysis of the Pd-hydride cycle was the rate limiting step
- A ranking of experiments approach improved kinetic parameter estimability

ACCEPTED MANUSCRIPT